Supplementary File for the Paper "MIMO Capacity Analysis and Channel Estimation for Electromagnetic Information Theory"

I. Proof of Proposition 2

The proof is based on the variational characterization of the eigenvalues of a positive semi-definite operator $T \succeq 0$ (also known as the Courant–Fischer–Weyl min-max principle) on a Hilbert space $\mathcal{H}$. Let $\lambda_k(T)$ be the k-th ($k \geq 0$) largest eigenvalue of T. Then, the variational characterization reads

$$\lambda_k(T) = \sup_{\mathcal{X}^{k+1} \subset \mathcal{H}} \inf_{f \in \mathcal{X}^{k+1} : \|f\|_2 = 1} \langle f, Tf \rangle, \tag{S1}$$

where $\mathcal{X}^{k+1}$ runs over all $(k+1)$-dimensional subspaces of $\mathcal{H}$. Using this variational characterization, for two positive semi-definite operators $T, W \succeq 0$, we have

$$\begin{aligned}
&\lambda_k(T+W) \\
&= \sup_{\mathcal{X}^{k+1} : \mathcal{X}^{k+1} \subset \mathcal{H}} \inf_{f \in \mathcal{X}^{k+1} : \|f\|_2 = 1} (\langle f, Tf \rangle + \langle f, Wf \rangle) \\
&\geq \sup_{\mathcal{X}^{k+1} : \mathcal{X}^{k+1} \subset \mathcal{H}} \inf_{f \in \mathcal{X}^{k+1} : \|f\|_2 = 1} \langle f, Tf \rangle \\
&= \lambda_k(T), \quad \forall\, k = 0, 1, 2, \cdots .
\end{aligned}$$

Since $T_Q : \mathcal{H}_1 \to \mathcal{H}_2$ is a contraction operator, for all $f \in \mathcal{H}_1$, we have

$$\langle f, (I - T_Q^\dagger T_Q) f \rangle = \|f\|_2^2 - \|T_Q f\|_2^2 \geq 0. \tag{S2}$$

This implies that the operator $W := I - T_Q^\dagger T_Q$ is positive semi-definite. Using (S2), we have

$$\begin{aligned}
\sigma_k^2(T_Q T_h) &= \lambda_k(T_h^\dagger T_Q^\dagger T_Q T_h) = \lambda_k(T_h^\dagger (I - W) T_h) \\
&\leq \lambda_k(T_h^\dagger T_h) = \sigma_k^2(T_h).
\end{aligned} \tag{S3}$$

By noticing that $\sigma_k(T) = \sigma_k(T^\dagger)$, we have

$$\begin{aligned}
\sigma_k^2(T_Q T_h T_P) &= \sigma_k^2(T_P^\dagger T_h^\dagger T_Q^\dagger) \\
&\leq \sigma_k^2(T_h^\dagger T_Q^\dagger) = \sigma_k^2(T_Q T_h) \\
&\leq \sigma_k^2(T_h), \quad \forall\, k = 0, 1, 2, \cdots .
\end{aligned} \tag{S4}$$

This completes the proof.

II. PSWF Bounds for H-MIMO and XL-MIMO in the Low SNR Regime

In this section, we check the behavior of the PSWF bound as a function of different SNR values P_T/σ_z^2 and different Tx/Rx aperture values L. All the other parameters are the same as those in the main text. Fig. S1 shows the normalized ergodic capacity of H-MIMO systems with an SNR of $3\,\mathrm{dB}$. Compared with the curves in Fig. 2 of the main document, it is shown that the PSWF bound is tighter in the low SNR regime. The same conclusion can be drawn from Fig. S3.

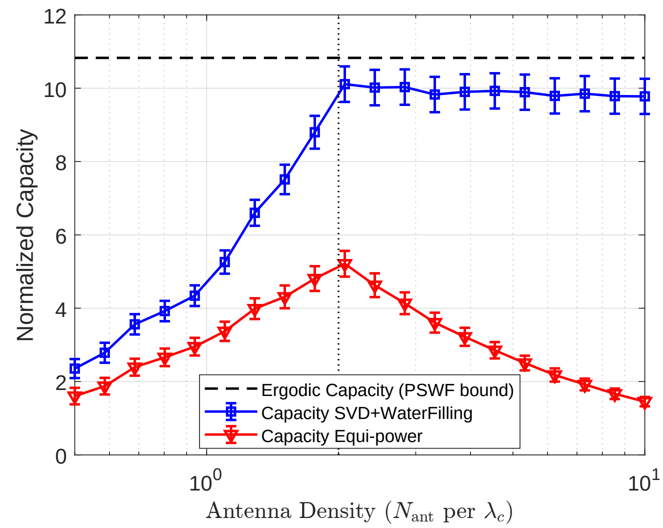

Fig. S1. The ergodic capacity saturation phenomenon of H-MIMO with $L_t = L_r = 1\,\mathrm{m}$, $P_\mathrm{T}/\sigma_z^2 = 3\,\mathrm{dB}$, and the number of Monte Carlo trials is 300.

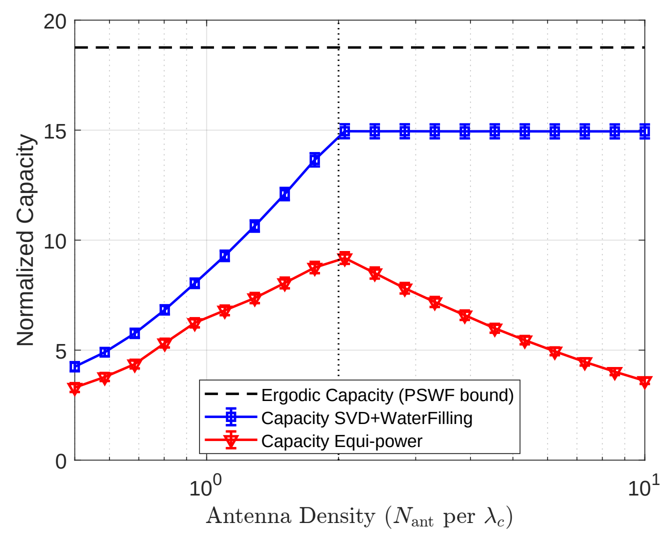

Fig. S2. The ergodic capacity saturation phenomenon of H-MIMO with $L_t = L_r = 2\,\mathrm{m}$, $P_\mathrm{T}/\sigma_z^2 = 10\,\mathrm{dB}$, and the number of Monte Carlo trials is 300.

Fig. S2 shows the normalized ergodic capacity of H-MIMO systems with enlarged aperture $L = 2\,\mathrm{m}$ and SNR of $10\,\mathrm{dB}$. Although larger apertures result in smaller standard deviations of the simulated capacity (via Monte Carlo trials), the PSWF bound is less accurate when the aperture increases.

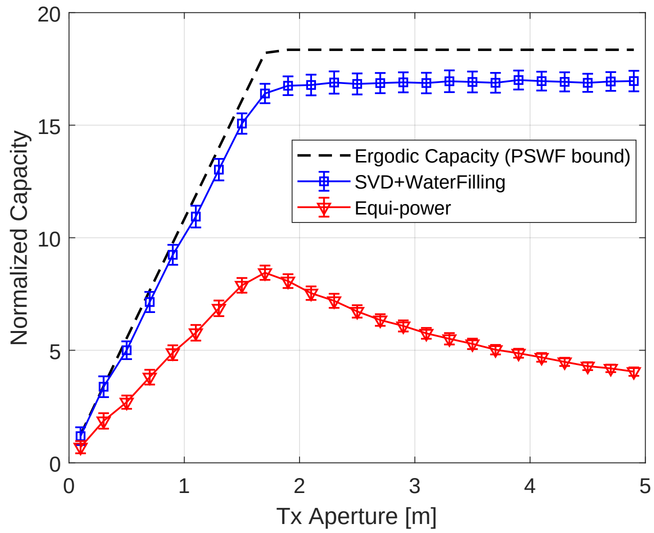

Fig. S3. The ergodic capacity saturation phenomenon of XL-MIMO with $P_{\mathrm{T}}/\sigma_z^2 = 3\,\mathrm{dB}$, and the number of Monte Carlo trials is 300.

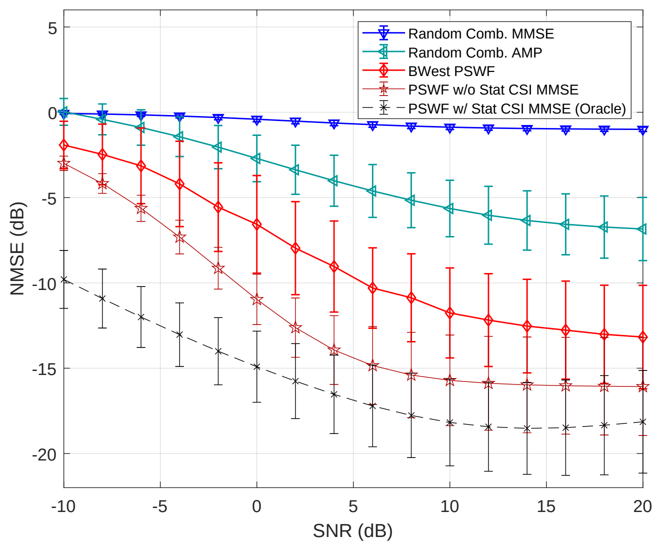

Fig. S4. The NMSE performance of MIMO channel estimators with aperture $L_t = L_r = 1.0\,[\mathrm{m}]$, $N_{\mathrm{P}} = 120$, and TR 38.901 CDL-A standardized channel. The number of Monte Carlo trials is 200.

III. Simulation of PSWF-CE with Standardized CDL Channels

In this supplementary section, we present performance of the simulated estimator PSWF-CE on the 3GPP TR 38.901 standardized channel model with delay profile CDL-A [1] (NLoS urban communication scenarios). For the MMSE channel estimator baseline, the channel covariance $\mathbf{C}_{\mathbf{h}}$ is approximated as

$$\mathbf{C}_{\mathbf{h}} \approx \frac{1}{N_{\mathrm{sim}} - 1} \sum_{n=1}^{N_{\mathrm{sim}}} \mathbf{h}_n \mathbf{h}_n^{\mathsf{H}}, \tag{S5}$$

where in our simulations we set $N_{\mathrm{sim}} = 10,000$, and $\mathbf{h}_n$ is the n–th realization of the CDL channel. Apart from the channel generation procedure, other settings are the same as those in the main text. Note that the CDL channel does not prefer our proposed PSWF-CE method.

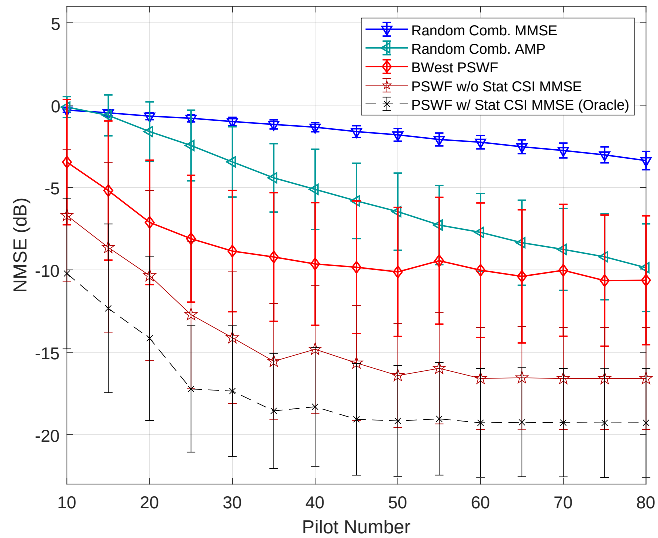

Fig. S5. The NMSE performance of MIMO channel estimators with respect to the pilot number N_{P}. The Tx/Rx aperture is $L_t = L_r = 0.5\,[\mathrm{m}]$, $\mathrm{SNR} = 20\,\mathrm{dB}$, and the number of Monte Carlo trials is 200.

In Fig. S4 and Fig. S5, the traditional MMSE estimators and compressed sensing-based approximate message passing (AMP) [2] estimators are compared with the proposed PSWF-CE estimators. The CDL channel generation implemented by the MATLAB 5G NR Toolbox. All the other settings are the same as those in Fig. 5 in the main document. From Fig. S4 and S5, we observe that the proposed PSWF-based estimators outperform the MMSE and AMP baselines on this real-world channel model. The oracle PSWF method exhibits a non-monotonic behavior due mainly to the inaccurate channel statistics estimation in Eqn. (S5). Since the CDL-A channel is more sparse than that adopted in Fig. 5, the AMP baseline is slightly improved. Thanks to the better channel representation enabled by PSWFs, the PSWF-based estimators still outperform AMP.

References

[1] *Study on channel model for frequencies from 0.5 to 100 GHz (Release 16) v16.1.0*, 3GPP TR 38.901 TSG RAN; NR, Dec. 2019.

[2] D. L. Donoho, A. Maleki, and A. Montanari, “Message passing algorithms for compressed sensing: I. motivation and construction,” in *Proc. IEEE Inf. Theory Workshop (ITW’10)*. IEEE, Jul. 2010, pp. 1–5.